Environmental Research 239 (2023) 117344

Contents lists available at ScienceDirect

Environmental Research

journal homepage: www.elsevier.com/locate/envres

Bromine, iodine and sodium along the EAIIST traverse: Bulk and surface snow latitudinal variability

G. Celli [a], W.R.L. Cairns [a,b], C. Scarchilli [c], C.A. Cuevas [d], A. Saiz-Lopez [d], J. Savarino [e], B. Stenni [a], M. Frezzotti [f], S. Becagli [g,b], B. Delmonte [h], H. Angot [e], R.P. Fernandez [i], A. Spolaor [a,b,*]

[a] Ca'Foscari University of Venice, Department of Environmental Sciences, Informatics and Statistics, Via Torino 155, 30172, Venice, Mestre, Italy
[b] CNR-Institute of Polar Sciences (CNR-ISP), 155 Via Torino, 30172, Venice, Mestre, Italy
[c] Department of Science, University of Roma Tre, Largo S. Leonardo Murialdo, 1, 00146, Roma, Italy
[d] Department of Atmospheric Chemistry and Climate, Institute of Physical Chemistry Rocasolano, IQFR-CSIC, 28006, Madrid, Spain
[e] Univ. Grenoble Alpes, CNRS, INRAE, IRD, Grenoble INP, IGE, 38000, Grenoble, France
[f] ENEA, C.R. Casaccia, 00123, Roma, Italy
[g] Department of Chemistry "Ugo Schiff", University of Florence, Sesto Fiorentino, Florence, 50019, Italy
[h] Department of Environmental Science, University of Milano-Bicocca, Milan, Italy
[i] Institute for Interdisciplinary Science, National Research Council (ICB-CONICET), FCEN-UNCuyo, Mendoza, 5501, Argentina

ARTICLE INFO

Keywords:
Antarctica
Halogens
Spatial distribution
Snowpack
Photochemistry

ABSTRACT

During the East Antarctic International Ice Sheet Traverse (Eaiist, december 2019), in an unexplored part of the East Antarctic Plateau, snow samples were collected to expand our knowledge of the latitudinal variability of iodine, bromine and sodium as well as their relation in connection with emission processes and photochemical activation in this unexplored area. A total of 32 surface (0–5 cm) and 32 bulk (average of 1 m depth) samples were taken and analysed by Inductively Coupled Plasma Mass Spectrometry (ICP-MS). Our results show that there is no relevant latitudinal trend for bromine and sodium. For bromine they also show that it has no significant post-depositional mechanisms while its inland surface snow concentration is influenced by spring coastal bromine explosions. Iodine concentrations are several orders of magnitude lower than bromine and sodium and they show a decreasing trend in the surface samples concentration moving southward. This suggests that other processes affect its accumulation in surface snow, probably related to the radial reduction in the ozone layer moving towards central Antarctica. Even though all iodine, bromine and sodium present similar long-range transport from the dominant coastal Antarctic sources, the annual seasonal cycle of the ozone hole over Antarctica increases the amount of UV radiation (in the 280–320 nm range) reaching the surface, thereby affecting the surface snow photoactivation of iodine. A comparison between the bulk and surface samples supports the conclusion that iodine undergoes spring and summer snow recycling that increases its atmospheric lifetime, while it tends to accumulate during the winter months when photochemistry ceases.

1. Introduction

Antarctica is considered a natural laboratory with unique atmospheric and climatological conditions. The Antarctic atmosphere is dry and dominated by cold temperatures. The solar cycle is characterised by periods of continuous daylight (from November to February), periods when the night and day cycle is present (from March to April and from September to October) and periods of polar night with 24 h of darkness (from May to August) (Hanson and Gordon, 1998). The Antarctic snowpack has been studied to investigate atmospheric depositions and transport processes, especially where instrumental data are unavailable, by exploring variations in concentration of indicator elements and compounds in the surface and buried snow (Proposito et al., 2002).

The role of iodine (I) in new particle formation as well as in the so-called tropospheric Ozone Depletion Events (ODEs) is currently under investigation since it could have a direct effect on the radiative budget of

* Corresponding author. Ca'Foscari University of Venice, Department of Environmental Sciences, Informatics and Statistics, Via Torino 155, 30172, Venice, Mestre, Italy.
E-mail address: andrea.spolaor@unive.it (A. Spolaor).

https://doi.org/10.1016/j.envres.2023.117344
Received 4 August 2023; Received in revised form 6 October 2023; Accepted 7 October 2023
Available online 10 October 2023

polar areas (Allan et al., 2015; Benavent et al., 2022; Gómez Martín et al., 2022; Raso et al., 2017; Saiz-Lopez et al., 2007b, 2012; Sipilä et al., 2016). The ocean is the main source of organic iodine compounds that are involved in complex atmospheric photoreactions leading to the formation of iodine atoms and iodine oxide (IO) (Saiz-Lopez et al., 2012). Iodine is mainly associated with biogenic emissions, which are 75% of the total IO budget (Prados-Roman et al., 2015), however, recent studies have highlighted especially in the North Atlantic ocean, an increase in oceanic inorganic iodine emissions (tripled since 1950) connected with increases in anthropogenic ozone via reactions over the ocean surface (Cuevas et al., 2018). Satellite and ground based measurements have revealed enhanced concentrations of atmospheric IO over the Antarctic coast (Mahajan et al., 2021; Saiz-Lopez et al., 2007a). Highest IO concentrations over sea-ice were observed in late spring when the atmosphere is photochemically activated. During the summer a second area of high IO concentrations was observed also over the Antarctica ice shelves (Schönhardt et al., 2008). Reduced forms of iodine (e.g., iodide (I^-) deposited as hydrogen iodide (HI)) deposit onto the snowpack where iodine is chemically active. In the upper snow layer, inorganic iodine can be released as volatile I_2 from the snowpack to the atmosphere after photo-oxidation (Raso et al., 2017; Spolaor et al., 2014). Researches performed at Law Dome, on the coast of East Antarctica, show a summer minimum of I in the snow when it is re-emitted due to the photochemical recycling of IO in the snowpack, and a winter peak during the night time of iodine when the IO recycling in the snowpack ceases (Spolaor et al., 2021). Repeated cycles of surface snow deposition and photo-emission of iodine can explain the inland migration of iodine in Antarctica (Spolaor et al., 2014). In the Arctic, the snowpack iodine cycle has been extensive studied and it has been found to follow a diurnal cycle, with concentrations peaking during the night and decreasing during the day (Spolaor et al., 2019).

Bromine (Br) is mainly released from the ocean and sea ice areas to the atmosphere via sea-salt aerosol (SSA) or as volatile short-lived organobromine species produced by ocean biota that are photolyzed in the atmosphere, where they react with ozone to produce BrO (Saiz-Lopez and Glasow, 2012). Satellite measurements show that BrO has its highest tropospheric concentration during springtime (from September to November) (Platt and Wagner, 1998), when seasonal sea-ice is present and biogenic emissions have not yet peaked. This is due to the autocatalytic release of BrO from heterogeneous reactions on the acidic sea-salt aerosols surface which, under particular circumstances, can have an exponential growth of gaseous reactive bromine, the so-called bromine explosion events (Frieß et al., 2004; Tang and McConnell, 1996). In the atmosphere BrO can be converted by atmospheric processes into HOBr and finally reacts in the snow with aqueous bromide (Br^-) to give gaseous Br_2 (Wang et al., 2019). This process has been suggested as an explanation for the bromine enrichment greater than the oceanic mass ratio of bromine and sodium (Br/Na) found in polar spring snow and it is used qualitatively to reconstruct past sea ice changes (Scoto et al., 2022). The release of bromine species from sea-salt aerosol, saline snow and a salty sea ice surface has a central role in controlling the ozone concentration in the lower troposphere during springtime ODEs (Barrie et al., 1988; Foster et al., 2001; Saiz-Lopez et al., 2007b, 2008; Simpson et al., 2007), which are largely defined by cyclic reactions between halogen radicals, their oxides and ozone (Platt and Hönninger, 2003; Wang et al., 2019).

Unlike the halogens, sodium is not photoreactive and is mainly emitted from the open ocean and the sea ice surface and then deposits onto the snowpack (Vallelonga et al., 2021). It is relatively easy to determine in ice and snow and can be used as a passive tracer for marine emissions and their deposition at a sampling site (Spolaor et al., 2013). Within the framework of the International Trans-Antarctic Scientific Expedition (ITASE), sodium showed a high spatial variability, decreasing with an initially exponential trend within the first 250 km from the coast before reaching a constant value further inland on the Antarctic ice sheet (Proposito et al., 2002). Bromine instead has a quasi-linear decreasing trend from the coast until almost 1000 km inland (Vallelonga et al., 2021).

In previous researches data on the occurrence of halogens in Antarctica were mainly restricted to coastal sites where the snow accumulation is sufficiently high to define the annual cycles. Maffezzoli et al. (2017) reported information on bromine, iodine and sodium from the Ross Sea to the Indian Ocean sector, in a 300 km traverse in the coastal area from Talos Dome to the GV7 site. They have detected a high variability for sodium and a springtime influence for bromine concentrations from the bromine explosion events at the coastal sites close to GV7, where the accumulation is highest. They reported that iodine had a low variability with an increase in values towards the coast (Maffezzoli et al., 2017). Other studies have investigated the Indian Ocean sector at Law Dome (Spolaor et al., 2014). Law Dome is directly influenced by the incursion of maritime air masses crossing over sea ice and being a high accumulation zone, it can preserve signals of seasonal cycles in the snowpack. Bromine and iodine have a clear seasonal variability, with iodine showing the highest concentration in winter ice core strata and bromine showing spring related peaks due to the bromine explosion events (Spolaor et al., 2014). In the Atlantic sector at Neumayer station measurements of BrO column have been made, investigating its correlation with the stratospheric ozone layer depletion and air masses movements (Frieβ et al., 2010). Multi-year atmospheric observations were made in East Antarctica on the coast (Dumont D'Urville (DDU) Station) and on the high plateau (Concordia Station, (Dome C)) (Legrand et al., 2016). They evaluated the aerosol composition for sea-salt and bromide depletion, and the snowpack content at Concordia to define possible bromine snow emissions. The results showed that snowpack bromine emissions were not important and that there was an unusual environmental conditions at DDU where sodium peaks in summer instead of in winter, as it happens elsewhere in the Antarctic coast (Legrand et al., 2016). More recent studies (Burgay et al., 2023; Spolaor et al., 2021) have investigated halogens chemistry in an ice core from Dome C. The main results showed that bromine is preserved in the snowpack (Burgay et al., 2023) while iodine geochemistry is influenced by the increased amount of solar radiation able to reach the Antarctic Plateau due to the ozone layer depletion (Spolaor et al., 2021).

The aim and the novelty of this paper is the understanding of the occurrence of iodine, sodium, and bromine in surface and bulk snow in an unexplored area of the East Antarctic plateau, starting from Dome C to the Megadune site (Fig. 1). We investigate their latitudinal distribution during the springtime, finding traces of air masses penetration from the ocean and a clear influence of spring bromine explosions in the bromine signal this far inside the Antarctic Plateau. The results are also supporting previous research on how iodine can behave in the snowpack surface with the sunlight and the potential impact of the ozone hole formation on the iodine geochemical cycle. Their possible seasonal accumulation processes are also investigated by comparing samples from the snowpack surface and from 1 m depth. This paper will particularly focus on transport and deposition processes and will examine how they are possibly influenced by specific environmental parameters that may control their preservation in the snowpack.

2. Sampling and analysis

2.1. Surface and bulk snow sampling

The samples were collected in East Antarctica during the East Antarctic International Ice Sheet Traverse (EAIIST) between December 2019 and January 2020, starting at the denominated site S1 about 40 km from Dome C (77°14′17.52″S, 123°28′35.34″E) and ending at the Mega Dune site, 678 km from Dome C, denominated as S32 (80°34′29.22″S, 121°43′55.80″E) (Fig. 1). Two typologies of snow samples were taken along the route at 32 sites (S1–S32), resulting in a total of 64 samples. At each sampling point, a 1-m bulk snow core was drilled using a dedicated drill, that was pre-cleaned before each sampling by drilling three

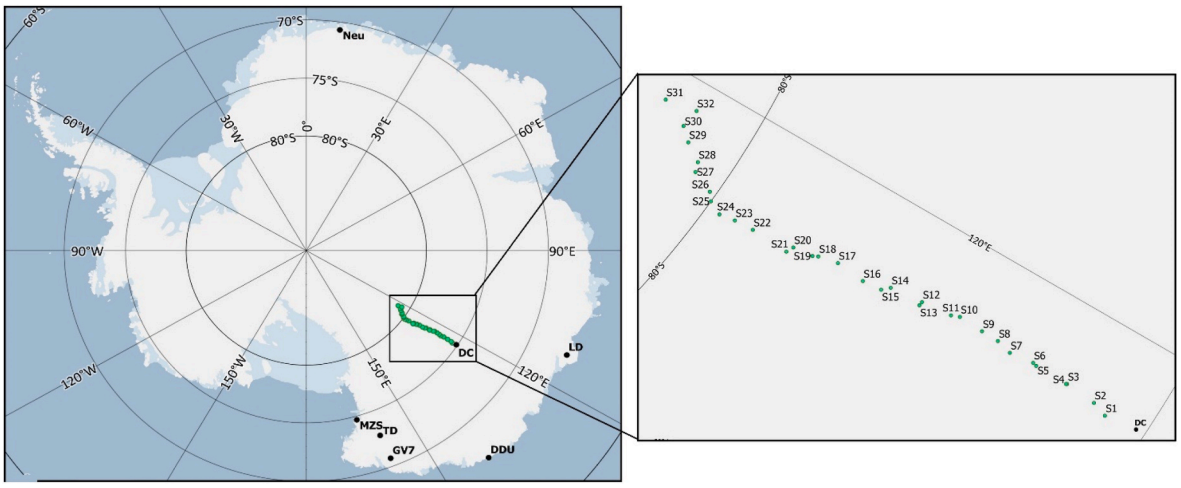

Fig. 1. Map of Antarctica showing the positions of the 32 sampling sites from Dome C (DC) station towards the South Pole (Map created with Quantarctica, Developed by the Norwegian Polar Institute). MZS stands for Mario Zucchelli station, DDU stands for Durmont d'Urville, TD stands for Talos Dome, GV7 stands for the GV7 site, LD stands for Law Dome and Neu stands for Neumayer station.

unsaved snow cores in the sampling location. The 1 m collected snow core was then homogenized inside a pre-cleaned plastic bag, and representative subsamples were taken for analysis. The 1 m bulk sample were collected to characterise the average deposition of each element at each specific site. Taking 1 m should cover at least 5 years of snow accumulation (based on the modelled average precipitation amount, Supplementary Fig. S1 and Table S2) and avoid possible artefacts due to short term meteorological events in the elements' deposition. Therefore, the bulk samples represent the average net deposition over a recent multi-annual period. At the same site, superficial snow was sampled from the first 5 cm of the snow layer, using sterile polypropylene tubes. Considering the snow accumulation rate at these sites (see supplementary information, Table S2), we considered the sampling depth (5 cm) to be representative of the most recent depositions that likely occurred during late winter and spring of year 2019. The samples were transported by the PNRA/IPEV Antarctic logistic stored in the dark at −20 °C. The same storage conditions were applied until analysis.

2.2. Samples chemical analysis

Concentrations of bromine, iodine, and sodium were determined by Inductively Coupled Plasma Mass Spectrometry (iCAP™ RQ ICP-MS; Thermo Scientific™) on an instrument fitted with a collision cell. All the analyses were done using the High Sensitivity insert (2.8 mm) and each sample determination consisted of three instrumental detections that were then averaged to provide the final quantification. More information about the standard deviation and the confidence interval can be found in Tables S3–S8 in the Supplementary material.

Samples were melted at room temperature in a class 1000 inorganic clean room under a class 100 laminar-flow bench. After each analytical run an ultra-pure water (UPW) cleaning session was run to test the cleanliness of the instrumental lines. The external standards used for the calibration were prepared gravimetrically. The 1000 parts per million (ppm) iodine and bromine standards for IC (Fluka® Analytical, Sigma-Aldrich) were diluted to produce three single element standards for iodine covering from 0.001 to 0.2 ng g^{-1} and three single element standards for bromine from 0.02 to 2 ng g^{-1}. The 1000 ppm sodium standard (Ultra Scientific, Analytical Solutions) was diluted to produce six standards from 2 to 100 ng g^{-1}. Detection limits, calculated as three times the standard deviation of the blank, were 0.0050 and 0.050 ng g^{-1} for I and Br respectively, and 0.80 ng g^{-1} for Na. Procedural UPW (Ultra Pure Water) blanks were analysed periodically to test the cleanliness of the instrument lines, and calibration standards were re-analysed every 20 samples as an additional quality control check.

2.3. Modeling of snow precipitation and ozone column

The modelled average precipitation at the sampling site was inferred from using the fifth generation European Centre for Medium-Range Weather Forecasts-Reanalysis (ECMWF ERA5) for the global climate and weather. ERA5 is a reanalysis based on the Integrated Forecasting System (IFS) model 204 cycle 41r2, that covers a period from 1979 to present and recently has been extended back in time up to 1950. The dataset for different meteorological and atmospheric physics variables is available on 37 pressure levels with a regular spatial grid of 0.25° × 0.25° at hourly temporal sampling (Guillory, 2022; Hersbach et al., 2020).

The total ozone column (TOC) over the region crossed by the EAIIST sampling traverse was calculated using the Community Earth System Model, version 1 (CESM1), with the WACCM4-SD as the atmospheric component configured in Specific Dynamic (SD) mode (Cuevas et al., 2022), with resolution of 2.5° longitude and 1.9° latitude. The model setup is based on the Chemistry-Climate Model Initiative (CCMI) configuration but nudging to the Modern Era Retrospective Analysis for Research and Applications (MERRA), meteorological dataset for the same period as the observation. The model is a fully coupled interactive chemistry climate model that also incorporates an updated halogen chemistry scheme for halogens and includes into the chemical scheme the Ox, NOx, HOx, ClOx, and BrOx chemical families. The scheme used in the model takes into consideration gas phase and heterogeneous reactions on aerosol particle and upper tropospheric ice crystals (Cuevas et al., 2022).

3. Results

Along the EAIIST traverse route (Fig. 1), sodium bulk snow concentrations are higher than surface concentrations, with an average of 67.9 ng g^{-1} and a standard deviation of 75.6 ng g^{-1} (67.9 ± 75.6 ng g^{-1}) (bulk) compared to 33.2 ± 25.8 ng g^{-1} (surface) respectively. Particularly, high concentrations were found in the first surface sample and the first two bulk samples closest to Dome C station where the concentrations rise to 147 ng g^{-1} for the surface sample and over 300 ng g^{-1} for the bulk samples. This is probably due to contamination from operation at Dome C station. Considering their high values with respect to the others points, these values have been removed from the plot in Fig. 2a. Apart from these first samples, Na has a stable concentration with no relevant latitudinal trend for both surface and bulk samples (Fig. 2a). To better visualise the difference in concentration between surface and bulk samples, we subtracted the bulk concentrations from the surface

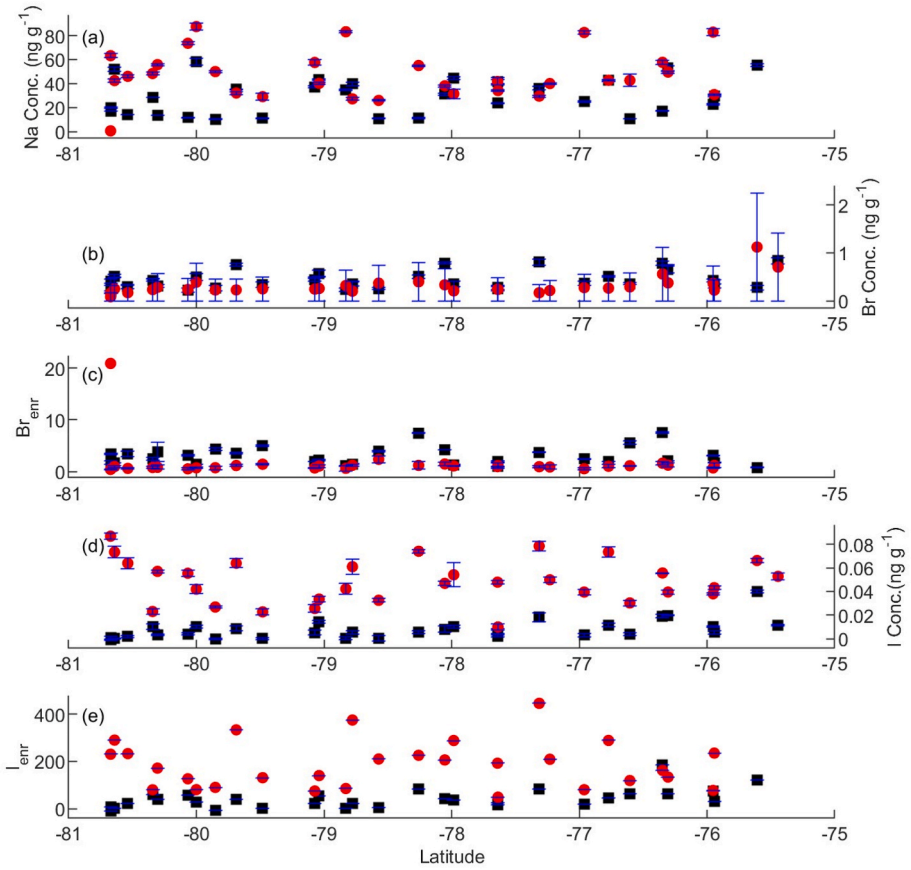

Fig. 2. Total surface and bulk concentrations at the 32 sampling sites for (a) Sodium (ng g^{-1}), (b) Bromine (ng g^{-1}), (c) Bromine enrichment, (d) Iodine (ng g^{-1}), (e) Iodine enrichment plotted against the latitude of the sampling site. The black squares represent the surface sample concentrations, the red dots the bulk sample concentrations. The error defined as the standard deviation is represented in blue.

concentrations (Fig. 3a). Applying this calculation, positive values indicate that the surface concentration is higher than the bulk concentration and negative values the converse.

Bromine has a surface average concentration of 0.4 ± 0.2 ng g^{-1} and a mean bulk concentration of 0.3 ± 0.2 ng g^{-1}. Fig. 2b shows that like sodium, bromine has the highest concentration close to Dome C Station, with a value of 1 ng g^{-1}. Moving southward Br shows no relevant trend in surface and bulk samples. Calculated differences between surface and bulk concentrations for Br are positive except for only four sites, meaning that bromine tends to accumulate into the surface samples (Fig. 3b). A similar behaviour is shown by the bromine enrichment (Br_{enr}) (Fig. 3c). The Br_{enr} calculated as the excess of bromine with respect to the oceanic mass ratio of bromine and sodium (Br/Na = 0.006) (Turekian, K. K., 1968), has a mean value of 2.9 ± 1.7 in the surface samples and 1.6 ± 0.4 in the bulk samples, where values > 1 indicate that Br is enriched in the samples compared to the marine abundance. Calculated differences between surface and bulk concentrations are positive, sign of a surface accumulation that agrees with the higher surface than bulk values of the Br_{enr}.

The Fig. 2d reports the iodine concentrations, where surface samples range from below the detection limit (0.0003 ng g^{-1}) to 0.04 ng g^{-1} with an average concentration of 0.006 ng g^{-1} ±0.006 ng g^{-1}. In the bulk samples, iodine concentrations range from 0.02 ng g^{-1} to 0.09 ng g^{-1} with an average concentration of 0.05 ng g^{-1} ± 0.02 ng g^{-1}. Calculated differences between surface and bulk concentrations for iodine are negative due to the higher bulk than surface concentration, implying an accumulation into the deeper part of the snowpack (Fig. 3d). As for Na and Br, iodine shows no relevant variation in the bulk samples along the sampling route. However, a decreasing latitudinal trend was observed for surface concentrations while moving southward from Dome C station.

To better understand the observed trends, we used normalized concentrations (Fig. 4) and evaluated their linear regression slope as shown in Tables 1 and 2. Data were normalized between 0 and 1, calculated with respect to their maximum and minimum concentration value. Final values of concentrations are now within the same range, and they can be directly compared including the trend in terms of absolute value of the regression line. As discussed above, iodine has the most relevant decreasing latitudinal surface trend for surface samples given by a higher negative slope than Br and Na where the trend is less pronounced.

4. Discussion

The results obtained suggest that neither sodium nor bromine have a north-south trend in surface and bulk snow in the explored area. Sodium has no photo-reactivity in the snow and is considered a sea-salt deposition proxy (Vallelonga et al., 2021). Despite the sampling sites being inland, previous researches (Jourdain et al., 2008; Legrand et al., 2016) have shown that sea-salt can travel for long distances from the sea-ice surface (Hara et al., 2004; Udisti et al., 2012) and reach the inland Antarctic Plateau. The stable/uniform surface concentration of sodium observed moving from Dome C Station to South Pole, implies a similar atmospheric sea spray transport regime for the region covered by the sampling campaign. The Dome C sector, where the EAIIST traverse took place, is mainly influenced by air masses coming from the Indian Ocean (Magand et al., 2004; Scarchilli et al., 2011; Sodemann and Stohl, 2009). The traverse route is in an area where the transport conditions and the air sources are considered constant, as evaluated in Scarchilli et al. (2011), with a back trajectory analysis for the East Antarctic area. It is well known that sodium accumulates in the snow with a seasonal cycle

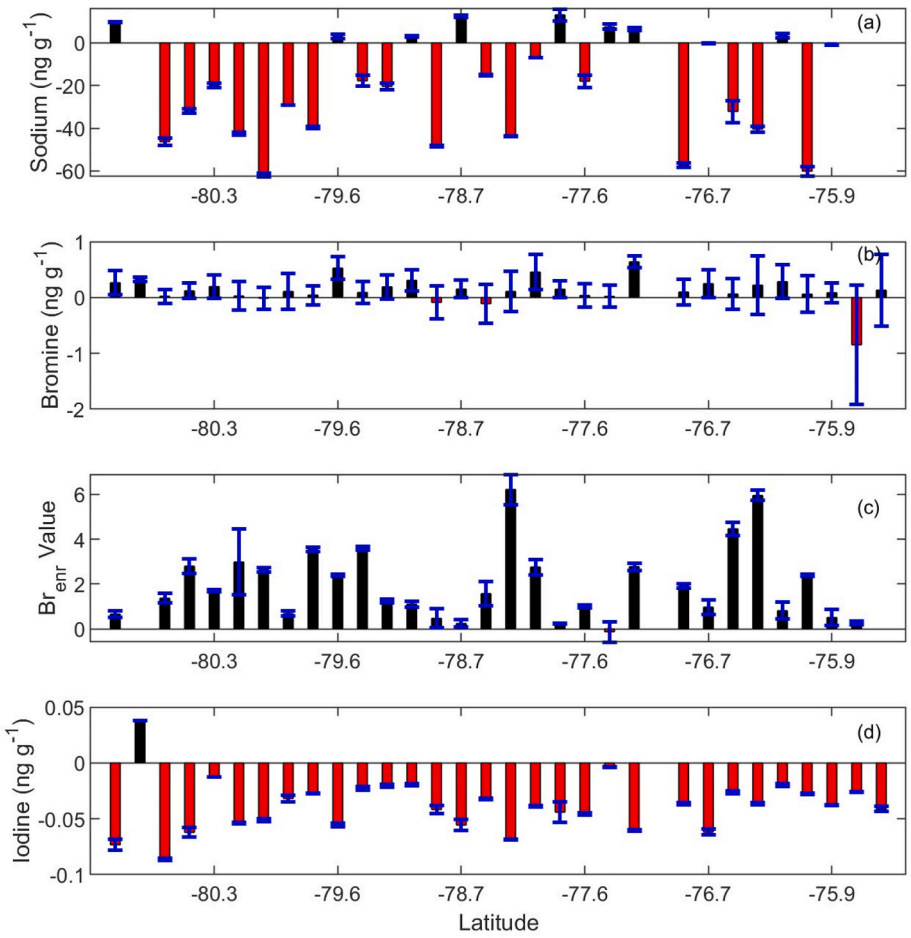

Fig. 3. Calculated differences between surface and bulk concentration of (a) Sodium, (b) Bromine, (c) Bromine Enrichment, (d) Iodine at each sampling-site. Positive differences in black when the surface concentration is higher and negative in red when the bulk concentration is higher. The error defined as the standard deviation is represented in blue.

peaking in winter (Legrand and Mayewski, 1997), indeed there is usually a higher winter concentration with large interannual variability (Legrand et al., 2016) which explains why bulk concentrations are higher than surface snow sampled in summer.

While it is well known that sodium is not affected by snow photochemistry, the snow stability of bromine is still uncertain. Modeling studies and empirical researches in the Arctic suggest a release of Br_2 from the sunlit surface snowpack, due to heterogeneous recycling of bromine species (Custard et al., 2017; Foster et al., 2001; Pratt et al., 2013) while others show a good snow stability (Spolaor et al., 2019; Thomas et al., 2011; Vallelonga et al., 2021). A recent study done at Dome C has demonstrated that in a 210 years record, the bromine signal is preserved and not affected by the strong variation in ultraviolet radiation reaching the snowpack due to the presence of the ozone hole (Burgay et al., 2023). In our results, bromine shows a similar trend to Na in surface snow, which is considered as a sign of a lack of post depositional photo-reactivity. However, there is still a debate in the scientific community on whether Br is stable after deposition or not. A comparison of Na and Br bulk and surface values, shows that while sodium has higher concentrations in the bulk samples, bromine has higher concentrations in the surface samples. We could explain this difference by assuming that the bulk samples represent years of snow accumulation, where their concentration values can be considered as mean annual values, while the surface samples are representative of the recent spring-summer depositions as already assumed for Na. Bromine can originate from the ocean surface (Saiz-Lopez and Glasow, 2012) and be transported together with Na in the sea-salt as well as in the gas phase. During springtime bromine explosion processes occur mainly over the sea ice. The snowpack (Peterson et al., 2018) acts as an additional seasonal source of this element in the polar atmosphere explaining the spring increase in surface snow concentrations (Frieβ et al., 2004). High mass ratio of Br/Na shows bromine enrichment relative to seawater ratio sea-salt during these events. Part of the sea-salt aerosol can be debrominated from salty blowing snow over the sea-ice in acidic conditions, releasing reactive bromine into the troposphere (Burgay et al., 2023). While sea salt is found in the atmosphere only as aerosol, halogens are also present in gaseous form. Gas-phase bromine (HOBr, BrO and Br_2) deposits via dry deposition processes and while it is transported from the sea-ice to the ice cap, it undergoes multiphase (aerosol-gas) chemical exchanges (Vallelonga et al., 2021). Comparing the sodium and bromine concentrations with bulk seawater concentrations allows us to define the bromine enrichment in ice and snow compared to the seawater abundance at the sampling sites (Vallelonga et al., 2021). With values greater than 1 the enrichments indicate an additional amount of bromine that cannot be attributed to sea-spray and might be correlated with other emission events such as spring bromine explosions. As seen on our results in Fig. 3b and c, higher values in Br and Br_{enr} in the upper snow layer relates to the springtime bromine explosions. A first evaluation of spatial variability of bromide in the snowpack was done up to 280 km inland from Utqiagvik (formerly known as Barrow station; northern Alaska), showing a gradual decrease or no decrease at all in bromide concentration, supporting the idea of an effective transport of recycled bromine inland (Simpson et al., 2005). Vallelonga et al. (2021) extends the research in Antarctica showing how the bromine concentration is

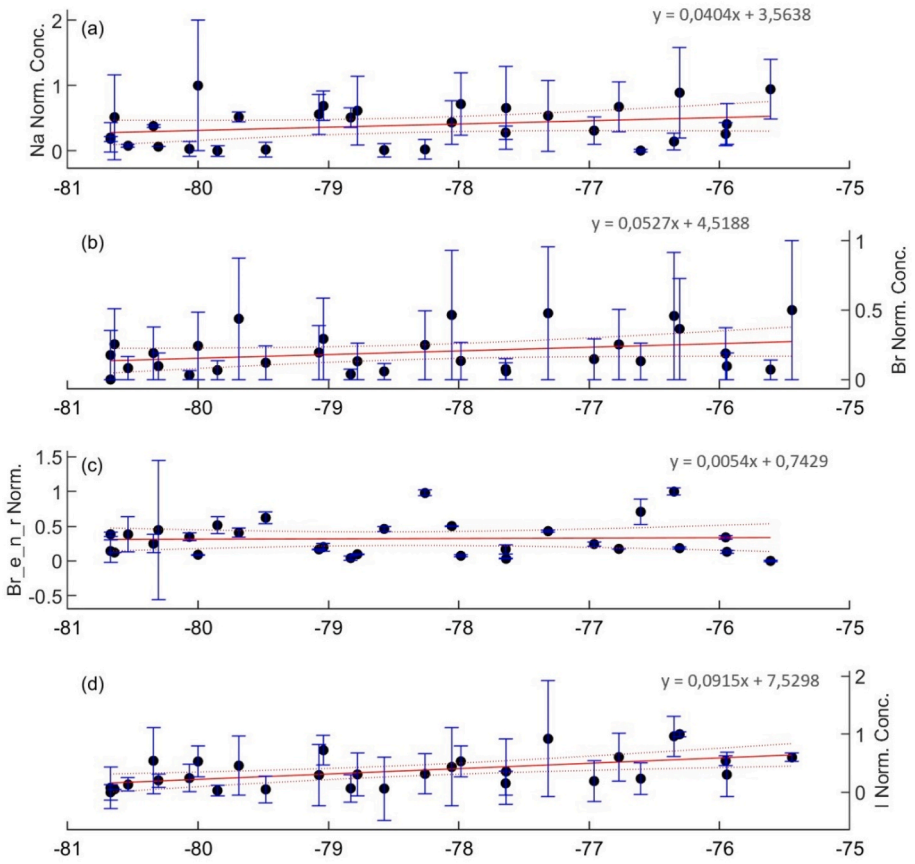

Fig. 4. Total surface normalized concentrations at the 32 sampling sites for (a) Sodium (ng g-1), (b) Bromine (ng g-1), (c) Bromine enrichment, (d) Iodine (ng g-1) plotted against the latitude of the sampling site. The black dots represent the surface sample concentrations, the red lines represent the linear regression and dashed red lines represent the confidence bounds defined with a level of certainty of 95%. The error defined as the standard deviation is represented in blue.

Table 1
Slope of the normalized bulk concentrations, with R squared, the Pearson coefficient of correlation (r) with its p-value (p). the slope error with its correlated *t*-test and p-value.

Analyte	Bulk Slope	R^2	r	p	Slope error	*t*-test	p
Bromine(Br)	0.059	0.30	0.54	0.014	0.050	2.95	0.006
Sodium(Na)	−0.015	0.006	−0.078	0.69	0.040	−0.10	0.92
Br Enrichment (Br_{enr})	0.040	0.094	0.31	0.11	0.026	1.57	0.13
Iodine (I)	−0.0088	0.0037	0.059	0.75	0.030	0.69	−0.071

Table 2
Slope of the normalized surface concentrations, with R squared, the Pearson coefficient of correlation (r) with its p-value (p). the slope error with its correlated *t*-test and p-value.

Analyte	Surface Slope	R^2	r	p	Slope error	*t*-test	p
Bromine(Br)	0.053	0.092	0.30	0.096	0.031	1.12	0.27
Sodium(Na)	0.040	0.044	0.21	0.27	0.034	0.60	0.55
Br Enrichment (Br_{enr})	0.0054	0.0012	0.084	0.35	0.031	0.64	0.53
Iodine (I)	0.091	0.29	0.54	0.0022	0.030	3.15	0.0040

usually low inside the continent and high at coastal sites where the influence of the marine environment is strong and how the Br_{enr} values are generally low at coastal locations and increase on the plateau. Our results agree with these previous studies that suggest that the Br seasonal cycle extends to the Antarctic plateau. Further observations during polar winter are needed to assess whether a bromine seasonality similar to that found in the coastal Antarctic Law Dome ice core (Spolaor et al., 2014) could also exist at Dome C.

Differently to sodium and bromine, iodine has a well-known snow photochemistry (Frieβ et al., 2010; Spolaor et al., 2014, 2019). Iodine undergoes snow photochemical processes driven by ultraviolet radiation in the bandwidth between 280 and 320 nm (Frieβ et al., 2010; Song et al., 2018; Spolaor et al., 2019, 2021). These wavelengths can convert this element from soluble ionic forms present in the snow, into gaseous forms, which are able to escape the snowpack and be re-emitted into the atmosphere. This process is limited by light penetration into the snowpack, and photochemical activation only occurs in the first 10–20 cm of the snowpack, a depth that depends on the snow physical properties (Simpson et al., 2002). No data are available yet in this specific area about albedo observation and/or light-absorbing snow properties, but

previous studies show no relevant changes of snow physical properties around Dome C, up to a northward distance of about 600 km, in this case towards DDU station (Gallet et al., 2011). Iodine concentration in surface snow shows different north-south trend compared to sodium and bromine. It shows a decreasing trend in surface snow moving south, a variation that is not visible in the bulk samples (Fig. 3d). The coast is the main source for iodine (Frieβ et al., 2010), as for sodium and bromine, but the trend differences suggest that other processes are acting on the surface snow concentration.

Snow accumulation could be one of the processes involved. However, as shown in Fig. S1 in the supplementary information, snow accumulation is low for all the sampling sites along the EAIIST traverse route. The traverse route is also located in a "rain-shadow area", defined as an area behind a mountainous region facing the non-prevailing wind side, where precipitation is significantly reduced. This so called "rain-shadow effect" is due to the trans Antarctic mountains and the east Antarctic ice cap, this in turn is responsible for a reduction of atmospheric moisture and precipitation penetration. Results obtained with the model presented above in section 2.3, show a low snow precipitation for all the sampling sites with a maximum value of 21 mm y^{-1} at site S2 and a minimum of 16 mm y^{-1} at site S14. From a general overview of the precipitation values, we do not see a trend from Dome C that can match the concentrations trend, and moreover, the few cm of precipitated snow that do occur remain in the photic zone for many years, until the snow accumulation reaches the 10/20 cm, the depth that the UV radiation can penetrate into the snow (France et al., 2011), which marks the depth available for photochemical processes due to light penetration.

As mentioned above, the trend for iodine could also be linked to changes in the source of the air masses or/and a progressive atmospheric depletion of this element moving south resulting in reduced depositions. However, this is not reflected in the Na and Br data, which do not show any decreasing concentration trend moving south. Moreover, the source strength effect can be removed considering the iodine enrichment. Both for surface and bulk samples values are above 1, ranging from 2 to 85 and from 25 to 446 respectively (Fig. 2e). One possible explanation for the iodine behaviour could be changes in UV radiation reaching the

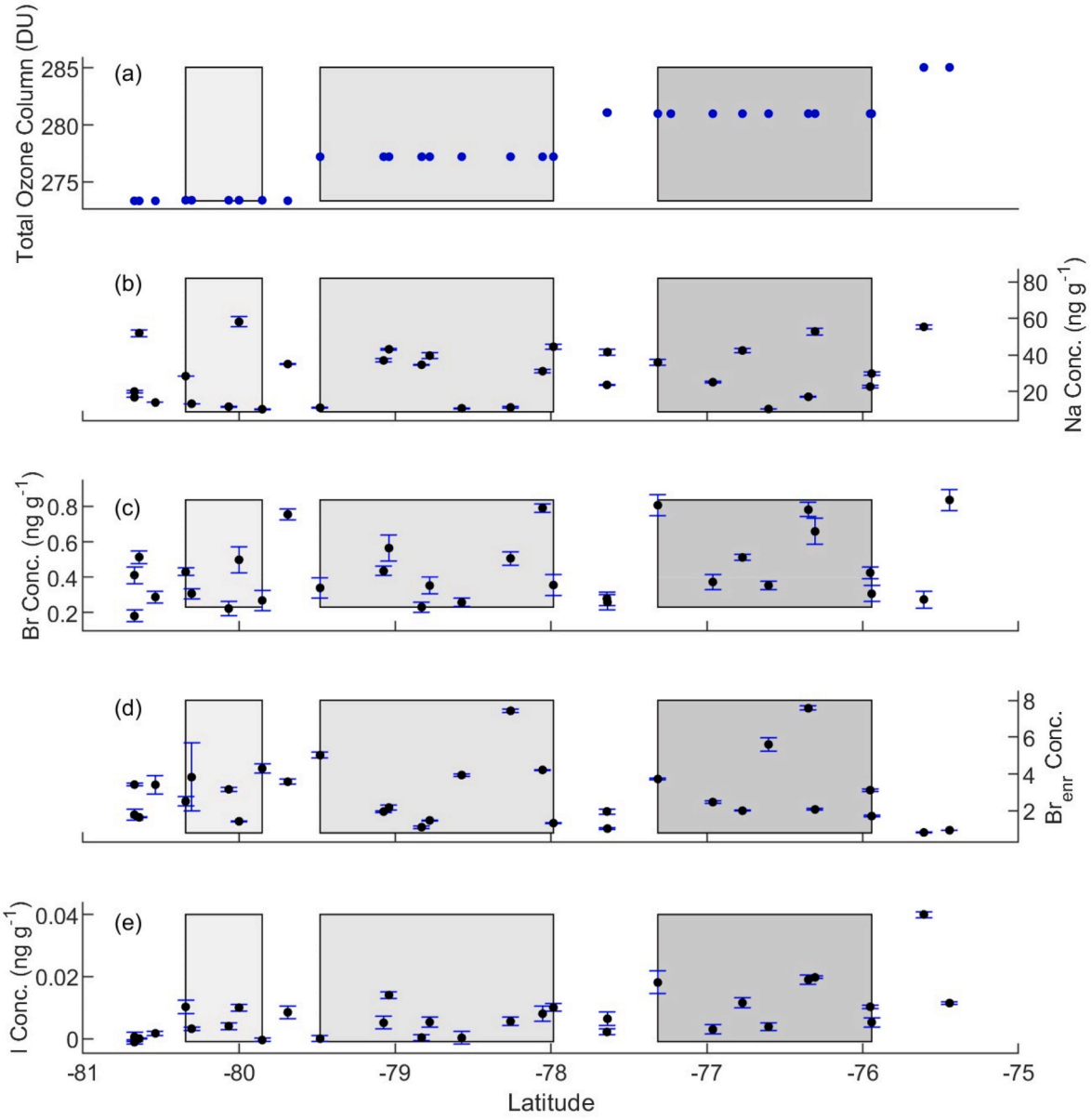

Fig. 5. (a) Modelled Total Ozone Column (TOC) in Dobson Unit (DU) over the EAIIST sampling site compared with the surface concentration at the sites of (b) bromine, (c) sodium, (d) bromine enrichment, (e) iodine. Grey areas represent constant TOC value for a group of sites near in latitude considered by the model into the same grid square with a spatial resolution of 1.9 degrees of latitude. The error defined as the standard deviation is represented in blue.

surface of the Antarctic Plateau connected with the formation of the ozone hole. The spring stratospheric ozone hole was discovered over Antarctica in the mid-1980s (Farman et al., 1985) as consequence of the massive use of chlorofluorocarbons (CFCs) (Rowland, 1990). The ozone layer completely absorbs the 220–290 nm component of solar radiation (Orphal et al., 2016) and partially absorbs the 290–320 nm band (Williamson et al., 2014). With the thinning of the ozone layer an increased amount of ultraviolet radiation reaches the Antarctic surface, with estimates of 80 to up to 400% more during maximum Antarctic ozone depletion (Brenna et al., 2019), particularly in the UV B range (Kerr and McElroy, 1993; Rowland, 1990). A link between iodine concentrations and ozone hole formation has already been suggested (Spolaor et al., 2021). In this study they found that the total ozone column (TOC) and the actinic flux (AF) showed a positive and a negative correlation respectively with the iodine snow concentration, in samples dated after 1975. This suggested a possible links between ozone hole formation, increased UV radiation and the promotion of iodine snow photochemistry and its subsequent release into the atmosphere. Following the same reasoning, the latitudinal trend that we observed in our iodine surface snow data, could be explained by changes in the thickness and shape of the ozone hole over the Antarctic continent. The depletion of the ozone layer is not uniform and is more pronounced in the interior of the continent and less so at the coast, following the seasonal formation of the polar stratospheric vortex. Values of TOC modelled as described above in section 2.3, show a decreasing trend in the TOC when moving further south from Dome C, from 285 to 273 DU respectively (Fig. 5a), similar to what we observed for iodine concentrations in the surface snow (Fig. 5e). We suggest that the surface latitudinal trend seen for I concentration in surface snow (Fig. 5e) could be linked to an increased amounts of UV B radiation reaching the snow surface due to the ozone layer depletion. This may promote the photo-reactivity of iodine in the photic zone of the snow leading to its higher re-emission from the snow surface, which could explain the lower surface concentrations observed (Fig. 5).

To explain the higher bulk compared to surface concentrations of iodine, we need to look at its seasonal behaviour. Our iodine observations are well supported by previous observations that indicate maximum iodine deposition into the snowpack in winter periods. Measurements from for the Law Dome Ice core (Spolaor et al., 2014) and from a snow pit at Neumayer station (Frieβ et al., 2010) have shown that iodine has a seasonal cycle, with winter peaks and summer values near or below the detection limit. Both of these sites are high accumulation sites with easily identifiable seasonal snow stratifications in which clear seasonal trends in iodine are found as a consequence of limited vertical migration after deposition (Frieβ et al., 2010). Their results show that iodine has a limited diffusivity in the snowpack and when it is photo-oxidised in the upper snow layer it is remitted exclusively into the atmosphere (Frieβ et al., 2010). During the polar night snow photochemistry ceases, and iodine can be deposited and preserved within the snowpack as it is buried before the polar sunrise (Spolaor et al., 2014). At low accumulation sites part of the winter iodine deposition remains in the photic zone and can be affected by UV radiation. This means that more than one year's worth of snow deposition may be necessary to preserve definitively the remaining iodine in low accumulation sites. This would explain our results of a higher bulk than surface concentrations. The iodine deposited in the first layer of the snowpack would be highly responsive to the ultraviolet radiation, while the iodine accumulated in the deeper snow, below the photic zone, is preserved. This is consistent with our results presenting a more pronounced latitudinal trend on surface snow iodine concentration than those observed for the bulk samples.

5. Conclusions

The 2019/2020 EAIIST traverse provided an opportunity to improve our knowledge about iodine and bromine latitudinal variations and their photo-reactivity on the East Antarctic Plateau. Compared to sodium concentrations, bromine in the surface samples is positively enriched compared to bromine in sea water, confirming the presence of spring bromine explosions and their transport inland. This enhances the amount of Br in the surface snow. For Na the stable surface trend indicates that air masses from the ocean have a stable pattern and a uniform sea-salt deposition, in the absence of specific air masses penetration. In addition, our Br results suggest net deposition to the snowpack. However, more studies are needed to clearly define this.

Even though post depositional photo-reactivity for iodine is well defined and surface snow samples show a clear latitudinal trend, our results cannot be fully explained, especially the difference in accumulation between surface and bulk samples, which could be linked to differences in snow diffusivity and atmospheric chemistry. Moreover, the variability along the transect follows the same decreasing trend as the ozone column as we move south over the sites in the sampling period. The sampling route coincided with the position of the ozone hole centre, where the ozone depletion is greatest, resulting in an increasing amount of UV radiation within the 280–320 nm range that has a strong influence on the surface concentration of this photo-reactive element. These results agree with the finding of Spolaor et al. (2021) about the connection between the ozone hole formation in 1975 and the iodine concentration variations in ice core samples from Dome C. Following this, the analysis of shallow core taken from some of the same sites as the surface and bulk samples, will be performed to identify a possible change into iodine concentrations before and after the ozone hole formation. This will also help us to define whether changes in the ozone column affect the snow-atmosphere exchange cycle of iodine, or whether there are specific mass transportation mechanisms that affect its deposition. This last hypothesis seems the least probable since the results for sodium and bromine show a uniform disposition along the traverse route.

The ice core analysis could also be used to integrate our bromine results to create a multi years data set for sea ice reconstruction. Sea ice dynamics are reconstructed by variations in Br and Br_{enr} concentrations (Vallelonga et al., 2021) and the bromine signal linked to sea ice extension is present and preserved at Dome C (Burgay et al., 2023). Considering this, we might be able to find information on the sea ice dynamic of the regions where the air masses that reach the Antarctic interior originate.

Experiments of photochemistry are also needed to investigate iodine lifetime in the snow and enhance the knowledge about the snow-atmosphere exchange mechanism with a focus on which iodine species is specifically involved, starting from previous investigations (Halfacre et al., 2019; Kim et al., 2016; Raso et al., 2017).

CRediT authorship contribution statement

G. Celli: Data curation, Formal analysis, Investigation, Methodology, Roles, Writing – original draft, Writing – review & editing. **W.R.L. Cairns:** Methodology, Supervision, Roles, Writing – original draft, Writing – review & editing, Formal analysis. **C. Scarchilli:** Writing – review & editing, Formal analysis. **C.A. Cuevas:** Writing – review & editing, Formal analysis. **A. Saiz-Lopez:** Writing – review & editing, Formal analysis. **J. Savarino:** Writing – review & editing, Funding acquisition, Project administration. **B. Stenni:** Writing – review & editing, Funding acquisition, Project administration. **M. Frezzotti:** Writing – review & editing, Project administration. **S. Becagli:** Writing – review & editing. **B. Delmonte:** Writing – review & editing. **H. Angot:** Writing – review & editing. **R.P. Fernandez:** Writing – review & editing, Formal analysis. **A. Spolaor:** Methodology, Supervision, Roles, Writing – original draft, Writing – review & editing, Formal analysis, Project administration, Funding acquisition.

Declaration of competing interest

The authors declare the following financial interests/personal

relationships which may be considered as potential competing interests: Barbara Stenni reports financial support, equipment, drugs, or supplies, and travel were provided by Programma Nazionale per la Ricerca in Antartide (PNRA, project number PNRA16_049). Joel Savarino reports financial support, equipment, drugs, or supplies, and travel were provided by Institut Polaire Français Paul Emile Victor. Joel Savarino reports financial support was provided by BNP-Paribas Climate Initiative programs. Joel Savarino reports financial support was provided by French National Research Agency.

Data availability

Data will be made available on request.

Acknowledgements

The authors would like to thank all the staff of the East International Ice sheet traverse that made possible the collection of the samples used in this manuscript. We also acknowledge all the logistical support received from the PNRA and IPEV for the safe samples handling, storage and transportation. This project received funding from the by the "Programma Nazionale per la Ricerca in Antartide" (PNRA, project number PNRA16_049).

Funding also provided by the Agence Nationale de la Recherche (ANR): ANR-10- LABX56, ANR-11-EQPX-009-CLIMCOR, ANR-16-CE01-0011-01 (J.S.), BNP-Paribas Climate Initiative programs (JS), and the Institut Polaire Français Paul Emile Victor programs: 1117 (CAPOXI 35–75) (JS) and 1169 (EAIIST) (J.S.).

Appendix A. Supplementary data

Supplementary data to this article can be found online at https://doi.org/10.1016/j.envres.2023.117344.

References

Allan, J.D., Williams, P.I., Najera, J., Whitehead, J.D., Flynn, M.J., Taylor, J.W., Liu, D., Darbyshire, E., Carpenter, L.J., Chance, R., Andrews, S.J., Hackenberg, S.C., McFiggans, G., 2015. Iodine observed in new particle formation events in the Arctic atmosphere during ACCACIA. Atmos. Chem. Phys. 15, 5599–5609. https://doi.org/10.5194/acp-15-5599-2015.

Barrie, L.A., Bottenheim, J.W., Schnell, R.C., Crutzen, P.J., Rasmussen, R.A., 1988. Ozone destruction and photochemical reactions at polar sunrise in the lower Arctic atmosphere. Nature 334, 138–141. https://doi.org/10.1038/334138a0.

Benavent, N., Mahajan, A.S., Li, Q., Cuevas, C.A., Schmale, J., Angot, H., Jokinen, T., Quéléver, L.L.J., Blechschmidt, A.-M., Zilker, B., Richter, A., Serna, J.A., Garcia-Nieto, D., Fernandez, R.P., Skov, H., Dumitrascu, A., Simões Pereira, P., Abrahamsson, K., Bucci, S., Duetsch, M., Stohl, A., Beck, I., Laurila, T., Blomquist, B., Howard, D., Archer, S.D., Bariteau, L., Helmig, D., Hueber, J., Jacobi, H.-W., Posman, K., Dada, L., Daellenbach, K.R., Saiz-Lopez, A., 2022. Substantial contribution of iodine to Arctic ozone destruction. Nat. Geosci. 15, 770–773. https://doi.org/10.1038/s41561-022-01018-w.

Brenna, H., Kutterolf, S., Krüger, K., 2019. Global ozone depletion and increase of UV radiation caused by pre-industrial tropical volcanic eruptions. Sci. Rep. 9, 9435. https://doi.org/10.1038/s41598-019-45630-0.

Burgay, F., Fernández, R.P., Segato, D., Turetta, C., Blaszczak-Boxe, C.S., Rhodes, R.H., Scarchilli, C., Ciardini, V., Barbante, C., Saiz-Lopez, A., Spolaor, A., 2023. 200-year ice core bromine reconstruction at Dome C (Antarctica): observational and modelling results. Cryosphere 17, 391–405. https://doi.org/10.5194/tc-17-391-2023.

Cuevas, C.A., Fernandez, R.P., Kinnison, D.E., Li, Q., Lamarque, J.-F., Trabelsi, T., Francisco, J.S., Solomon, S., Saiz-Lopez, A., 2022. The influence of iodine on the Antarctic stratospheric ozone hole. Proc. Natl. Acad. Sci. USA 119, e2110864119. https://doi.org/10.1073/pnas.2110864119.

Cuevas, C.A., Maffezzoli, N., Corella, J.P., Spolaor, A., Vallelonga, P., Kjær, H.A., Simonsen, M., Winstrup, M., Vinther, B., Horvat, C., Fernandez, R.P., Kinnison, D., Lamarque, J.-F., Barbante, C., Saiz-Lopez, A., 2018. Rapid increase in atmospheric iodine levels in the North Atlantic since the mid-20th century. Nat. Commun. 9, 1452. https://doi.org/10.1038/s41467-018-03756-1.

Custard, K.D., Raso, A.R.W., Shepson, P.B., Staebler, R.M., Pratt, K.A., 2017. Production and release of molecular bromine and chlorine from the arctic coastal snowpack. ACS Earth Space Chem. 1, 142–151. https://doi.org/10.1021/acsearthspacechem.7b00014.

Farman, J.C., Gardiner, B.G., Shanklin, J.D., 1985. Large losses of total ozone in Antarctica reveal seasonal ClOx/NOx interaction. Nature 315, 207–210. https://doi.org/10.1038/315207a0.

Foster, K.L., Plastridge, R.A., Bottenheim, J.W., Shepson, P.B., Finlayson-Pitts, B.J., Spicer, C.W., 2001. The role of Br2 and BrCl in surface ozone destruction at polar sunrise. Science 291, 471–474. https://doi.org/10.1126/science.291.5503.471.

France, J.L., King, M.D., Frey, M.M., Erbland, J., Picard, G., Preunkert, S., MacArthur, A., Savarino, J., 2011. Snow optical properties at Dome C (Concordia), Antarctica; implications for snow emissions and snow chemistry of reactive nitrogen. Atmos. Chem. Phys. 11, 9787–9801. https://doi.org/10.5194/acp-11-9787-2011.

Frieß, U., Deutschmann, T., Gilfedder, B.S., Weller, R., Platt, U., 2010. Iodine monoxide in the Antarctic snowpack. Atmos. Chem. Phys. 10, 2439–2456. https://doi.org/10.5194/acp-10-2439-2010.

Frieß, U., Hollwedel, J., König-Langlo, G., Wagner, T., Platt, U., 2004. Dynamics and chemistry of tropospheric bromine explosion events in the Antarctic coastal region. J. Geophys. Res. Atmos. 109 https://doi.org/10.1029/2003JD004133.

Gallet, J.-C., C, J., Domine, F., Arnaud, L., Picard, G., Savarino, J., 2011. Vertical profile of the specific surface area and density of the snow at Dome C and on a transect to Dumont D'Urville, Antarctica - albedo calculations and comparison to remote sensing products. Cryosphere 5, 631–649. https://doi.org/10.5194/tc-5-631-2011.

Gómez Martín, J.C., Lewis, T.R., James, A.D., Saiz-Lopez, A., Plane, J.M.C., 2022. Insights into the chemistry of iodine new particle formation: the role of iodine oxides and the source of iodic acid. J. Am. Chem. Soc. 144, 9240–9253. https://doi.org/10.1021/jacs.1c12957.

Guillory, A., 2022. ERA5 [WWW Document]. ECMWF. URL. https://www.ecmwf.int/en/forecasts/datasets/reanalysis-datasets/era5. (Accessed 16 March 2023).

Halfacre, J.W., Shepson, P.B., Pratt, K.A., 2019. pH-dependent production of molecular chlorine, bromine, and iodine from frozen saline surfaces. Atmos. Chem. Phys. 19, 4917–4931. https://doi.org/10.5194/acp-19-4917-2019.

Hanson, J.D., Gordon, J.E., 1998. In: Antarctic Environments and Resources, A Geographical Perspective, 1. Publ. Longman, Harlow.

Hara, K., Osada, K., Kido, M., Hayashi, M., Matsunaga, K., Iwasaka, Y., Yamanouchi, T., Hashida, G., Fukatsu, T., 2004. Chemistry of sea-salt particles and inorganic halogen species in Antarctic regions: compositional differences between coastal and inland stations. J. Geophys. Res. Atmos. 109 https://doi.org/10.1029/2004JD004713.

Hersbach, H., Bell, B., Berrisford, P., Hirahara, S., Horányi, A., Muñoz-Sabater, J., Nicolas, J., Peubey, C., Radu, R., Schepers, D., Simmons, A., Soci, C., Abdalla, S., Abellan, X., Balsamo, G., Bechtold, P., Biavati, G., Bidlot, J., Bonavita, M., De Chiara, G., Dahlgren, P., Dee, D., Diamantakis, M., Dragani, R., Flemming, J., Forbes, R., Fuentes, M., Geer, A., Haimberger, L., Healy, S., Hogan, R.J., Hólm, E., Janisková, M., Keeley, S., Laloyaux, P., Lopez, P., Lupu, C., Radnoti, G., de Rosnay, P., Rozum, I., Vamborg, F., Villaume, S., Thépaut, J.-N., 2020. The ERA5 global reanalysis. Q. J. R. Meteorol. Soc. 146, 1999–2049. https://doi.org/10.1002/qj.3803.

Jourdain, B., Preunkert, S., Cerri, O., Castebrunet, H., Udisti, R., Legrand, M., 2008. Year-round record of size-segregated aerosol composition in central Antarctica (Concordia station): implications for the degree of fractionation of sea-salt particles. J. Geophys. Res. Atmos. 113 https://doi.org/10.1029/2007JD009584.

Kerr, J.B., McElroy, C.T., 1993. Evidence for large upward trends of ultraviolet-B radiation linked to ozone depletion. Science 262, 1032–1034. https://doi.org/10.1126/science.262.5136.1032.

Kim, K., Yabushita, A., Okumura, M., Saiz-Lopez, A., Cuevas, C.A., Blaszczak-Boxe, C.S., Min, D.W., Yoon, H.-I., Choi, W., 2016. Production of molecular iodine and tri-iodide in the frozen solution of iodide: implication for polar atmosphere. Environ. Sci. Technol. 50, 1280–1287. https://doi.org/10.1021/acs.est.5b05148.

Legrand, M., Mayewski, P., 1997. Glaciochemistry of polar ice cores: a review. Rev. Geophys. 35, 219–243. https://doi.org/10.1029/96RG03527.

Legrand, M., Yang, X., Preunkert, S., Theys, N., 2016. Year-round records of sea salt, gaseous and particulate inorganic bromine in the atmospheric boundary layer at coastal (Dumont d'Urville) and central (Concordia) East Antarctic sites. J. Geophys. Res. Atmos. 121, 997–1023. https://doi.org/10.1002/2015JD024066.

Maffezzoli, N., Spolaor, A., Barbante, C., Bertò, M., Frezzotti, M., Vallelonga, P., 2017. Bromine, iodine and sodium in surface snow along the 2013 Talos Dome–GV7 traverse (northern Victoria Land, East Antarctica). Cryosphere 11, 693–705. https://doi.org/10.5194/tc-11-693-2017.

Magand, O., Frezzotti, M., Pourchet, M., Stenni, B., Genoni, L., Fily, M., 2004. Climate variability along latitudinal and longitudinal transects in East Antarctica. Ann. Glaciol. 39, 351–358. https://doi.org/10.3189/172756404781813961.

Mahajan, A.S., Biswas, M.S., Beirle, S., Wagner, T., Schönhardt, A., Benavent, N., Saiz-Lopez, A., 2021. Observations of iodine monoxide over three summers at the Indian Antarctic bases of Bharati and Maitri. Atmos. Chem. Phys. 21, 11829–11842. https://doi.org/10.5194/acp-21-11829-2021.

Orphal, J., Staehelin, J., Tamminen, J., Braathen, G., De Backer, M.-R., Bais, A., Balis, D., Barbe, A., Bhartia, P.K., Birk, M., Burkholder, J.B., Chance, K., von Clarmann, T., Cox, A., Degenstein, D., Evans, R., Flaud, J.-M., Flittner, D., Godin-Beekmann, S., Gorshelev, V., Gratien, A., Hare, E., Janssen, C., Kyrölä, E., McElroy, T., McPeters, R., Pastel, M., Petersen, M., Petropavlovskikh, I., Picquet-Varrault, B., Pitts, M., Labow, G., Rotger-Languereau, M., Leblanc, T., Lerot, C., Liu, X., Moussay, P., Redondas, A., Van Roozendael, M., Sander, S.P., Schneider, M., Serdyuchenko, A., Veefkind, P., Viallon, J., Viatte, C., Wagner, G., Weber, M., Wielgosz, R.I., Zehner, C., 2016. Absorption cross-sections of ozone in the ultraviolet and visible spectral regions: status report 2015. J. Mol. Spectrosc., New Visions of Spectrosc. Databases, Volume II 327, 105–121. https://doi.org/10.1016/j.jms.2016.07.007.

Peterson, P.K., Pöhler, D., Zielcke, J., General, S., Frieß, U., Platt, U., Simpson, W.R., Nghiem, S.V., Shepson, P.B., Stirm, B.H., Pratt, K.A., 2018. Springtime bromine

activation over coastal and inland arctic snowpacks. ACS Earth Space Chem. 2, 1075–1086. https://doi.org/10.1021/acsearthspacechem.8b00083.
Platt, U., Hönninger, G., 2003. The role of halogen species in the troposphere. Chem. Nat. Produced Organohalogens 52, 325–338. https://doi.org/10.1016/S0045-6535(03)00216-9.
Platt, U., Wagner, T., 1998. Satellite mapping of enhanced BrO concentrations in the troposphere. Nature 395, 486–490. https://doi.org/10.1038/26723.
Prados-Roman, C., Cuevas, C.A., Hay, T., Fernandez, R.P., Mahajan, A.S., Royer, S.-J., Galí, M., Simó, R., Dachs, J., Großmann, K., Kinnison, D.E., Lamarque, J.-F., Saiz-Lopez, A., 2015. Iodine oxide in the global marine boundary layer. Atmos. Chem. Phys. 15, 583–593. https://doi.org/10.5194/acp-15-583-2015.
Pratt, K.A., Custard, K.D., Shepson, P.B., Douglas, T.A., Pöhler, D., General, S., Zielcke, J., Simpson, W.R., Platt, U., Tanner, D.J., Gregory Huey, L., Carlsen, M., Stirm, B.H., 2013. Photochemical production of molecular bromine in Arctic surface snowpacks. Nat. Geosci. 6, 351–356. https://doi.org/10.1038/ngeo1779.
Proposito, M., Becagli, S., Castellano, E., Flora, O., Genoni, L., Gragnani, R., Stenni, B., Traversi, R., Udisti, R., Frezzotti, M., 2002. Chemical and isotopic snow variability along the 1998 ITASE traverse from terra nova bay to Dome C, east Antarctica. Ann. Glaciol. 35, 187–194. https://doi.org/10.3189/172756402781817167.
Raso, A.R.W., Custard, K.D., May, N.W., Tanner, D., Newburn, M.K., Walker, L., Moore, R.J., Huey, L.G., Alexander, L., Shepson, P.B., Pratt, K.A., 2017. Active molecular iodine photochemistry in the Arctic. Proc. Natl. Acad. Sci. USA 114, 10053–10058. https://doi.org/10.1073/pnas.1702803114.
Rowland, F.S., 1990. Stratospheric ozone depletion by chlorofluorocarbons. Ambio 19, 281–292.
Saiz-Lopez, A., Chance, K., Liu, X., Kurosu, T.P., Sander, S.P., 2007a. First observations of iodine oxide from space. Geophys. Res. Lett. 34 https://doi.org/10.1029/2007GL030111.
Saiz-Lopez, A., Glasow, R. von, 2012. Reactive halogen chemistry in the troposphere. Chem. Soc. Rev. 41, 6448–6472. https://doi.org/10.1039/C2CS35208G.
Saiz-Lopez, A., Mahajan, A.S., Salmon, R.A., Bauguitte, S.J.-B., Jones, A.E., Roscoe, H.K., Plane, J.M.C., 2007b. Boundary layer halogens in coastal Antarctica. Science 317, 348–351. https://doi.org/10.1126/science.1141408.
Saiz-Lopez, A., Plane, J.M.C., Baker, A.R., Carpenter, L.J., von Glasow, R., Gómez Martín, J.C., McFiggans, G., Saunders, R.W., 2012. Atmospheric chemistry of iodine. Chem. Rev. 112, 1773–1804. https://doi.org/10.1021/cr200029u.
Saiz-Lopez, A., Plane, J.M.C., Mahajan, A.S., Anderson, P.S., Bauguitte, S.J.-B., Jones, A.E., Roscoe, H.K., Salmon, R.A., Bloss, W.J., Lee, J.D., Heard, D.E., 2008. On the vertical distribution of boundary layer halogens over coastal Antarctica: implications for O_3, HO_x, NO_x and the Hg lifetime. Atmos. Chem. Phys. 8, 887–900. https://doi.org/10.5194/acp-8-887-2008.
Scarchilli, C., Frezzotti, M., Ruti, P.M., 2011. Snow precipitation at four ice core sites in East Antarctica: provenance, seasonality and blocking factors. Clim. Dynam. 37, 2107–2125. https://doi.org/10.1007/s00382-010-0946-4.
Schönhardt, A., Richter, A., Wittrock, F., Kirk, H., Oetjen, H., Roscoe, H.K., Burrows, J.P., 2008. Observations of iodine monoxide columns from satellite. Atmos. Chem. Phys. 8, 637–653. https://doi.org/10.5194/acp-8-637-2008.
Scoto, F., Sadatzki, H., Maffezzoli, N., Barbante, C., Gagliardi, A., Varin, C., Vallelonga, P., Gkinis, V., Dahl-Jensen, D., Kjær, H.A., Burgay, F., Saiz-Lopez, A., Stein, R., Spolaor, A., 2022. Sea ice fluctuations in the Baffin Bay and the Labrador Sea during glacial abrupt climate changes. Proc. Natl. Acad. Sci. USA 119, e2203468119. https://doi.org/10.1073/pnas.2203468119.
Simpson, W.R., Alvarez-Aviles, L., Douglas, T.A., Sturm, M., Domine, F., 2005. Halogens in the coastal snow pack near Barrow, Alaska: evidence for active bromine air-snow chemistry during springtime. Geophys. Res. Lett. 32, L04811 https://doi.org/10.1029/2004GL021748.
Simpson, W.R., King, M.D., Beine, H.J., Honrath, R.E., Zhou, X., 2002. Radiation-transfer modeling of snow-pack photochemical processes during ALERT 2000. Atmospheric environment, air/snow/ice interactions in the arctic: results from ALERT 2000 and. Summit 36, 2663–2670. https://doi.org/10.1016/S1352-2310(02)00124-3, 2000.
Simpson, W.R., von Glasow, R., Riedel, K., Anderson, P., Ariya, P., Bottenheim, J., Burrows, J., Carpenter, L.J., Frieß, U., Goodsite, M.E., Heard, D., Hutterli, M., Jacobi, H.-W., Kaleschke, L., Neff, B., Plane, J., Platt, U., Richter, A., Roscoe, H., Sander, R., Shepson, P., Sodeau, J., Steffen, A., Wagner, T., Wolff, E., 2007. Halogens and their role in polar boundary-layer ozone depletion. Atmos. Chem. Phys. 7, 4375–4418. https://doi.org/10.5194/acp-7-4375-2007.
Sipilä, M., Sarnela, N., Jokinen, T., Henschel, H., Junninen, H., Kontkanen, J., Richters, S., Kangasluoma, J., Franchin, A., Peräkylä, O., Rissanen, M.P., Ehn, M., Vehkamäki, H., Kurten, T., Berndt, T., Petäjä, T., Worsnop, D., Ceburnis, D., Kerminen, V.-M., Kulmala, M., O'Dowd, C., 2016. Molecular-scale evidence of aerosol particle formation via sequential addition of HIO3. Nature 537, 532–534. https://doi.org/10.1038/nature19314.
Sodemann, H., Stohl, A., 2009. Asymmetries in the moisture origin of Antarctic precipitation. Geophys. Res. Lett. 36 https://doi.org/10.1029/2009GL040242.
Song, S., Angot, H., Selin, N., Gallée, H., Sprovieri, F., Pirrone, N., Helmig, D., Savarino, J., Magand, O., Dommergue, A., 2018. Understanding mercury oxidation and air-snow exchange on the East Antarctic Plateau: a modeling study. Atmos. Chem. Phys. 18, 15825–15840. https://doi.org/10.5194/acp-18-15825-2018.
Spolaor, A., Barbaro, E., Cappelletti, D., Turetta, C., Mazzola, M., Giardi, F., Björkman, M., Lucchetta, F., Dallo, F., Pfaffhuber, K.A., Angot, H., Dommergue, A., Maturilli, M., Alfonso, S.-L., Barbante, C., Cairns, W., 2019. Diurnal cycle of iodine, bromine, and mercury concentrations in Svalbard surface snow. Atmos. Chem. Phys. 19, 13325–13339. https://doi.org/10.5194/acp-19-13325-2019.
Spolaor, A., Burgay, F., Fernandez, R.P., Turetta, C., Cuevas, C.A., Kim, K., Kinnison, D.E., Lamarque, J.-F., de Blasi, F., Barbaro, E., Corella, J.P., Vallelonga, P., Frezzotti, M., Barbante, C., Saiz-Lopez, A., 2021. Antarctic ozone hole modifies iodine geochemistry on the Antarctic Plateau. Nat. Commun. 12, 5836. https://doi.org/10.1038/s41467-021-26109-x.
Spolaor, A., Vallelonga, P., Gabrieli, J., Martma, T., Björkman, M.P., Isaksson, E., Cozzi, G., Turetta, C., Kjær, H.A., Curran, M.a.J., Moy, A.D., Schönhardt, A., Blechschmidt, A.-M., Burrows, J.P., Plane, J.M.C., Barbante, C., 2014. Seasonality of halogen deposition in polar snow and ice. Atmos. Chem. Phys. 14, 9613–9622. https://doi.org/10.5194/acp-14-9613-2014.
Spolaor, A., Vallelonga, P., Plane, J.M.C., Kehrwald, N., Gabrieli, J., Varin, C., Turetta, C., Cozzi, G., Kumar, R., Boutron, C., Barbante, C., 2013. Halogen species record Antarctic sea ice extent over glacial–interglacial periods. Atmos. Chem. Phys. 13, 6623–6635. https://doi.org/10.5194/acp-13-6623-2013.
Tang, T., McConnell, J.C., 1996. Autocatalytic release of bromine from Arctic snow pack during polar sunrise. Geophys. Res. Lett. 23, 2633–2636. https://doi.org/10.1029/96GL02572.
Thomas, J.L., Stutz, J., Lefer, B., Huey, L.G., Toyota, K., Dibb, J.E., von Glasow, R., 2011. Modeling chemistry in and above snow at Summit, Greenland – Part 1: model description and results. Atmos. Chem. Phys. 11, 4899–4914. https://doi.org/10.5194/acp-11-4899-2011.
Turekian, K.K., 1968. Oceans. Prenitce-Hall, New Jersey.
Udisti, R., Dayan, U., Becagli, S., Busetto, M., Frosini, D., Legrand, M., Lucarelli, F., Preunkert, S., Severi, M., Traversi, R., Vitale, V., 2012. Sea spray aerosol in central Antarctica. Present atmospheric behaviour and implications for paleoclimatic reconstructions. Atmos. Environ. Phys. chem. optical and radiative properties of polar aerosols – IPY 2007 - 2008 52, 109–120. https://doi.org/10.1016/j.atmosenv.2011.10.018.
Vallelonga, P., Maffezzoli, N., Saiz-Lopez, A., Scoto, F., Kjær, H.A., Spolaor, A., 2021. Sea-ice reconstructions from bromine and iodine in ice cores. Quat. Sci. Rev. 269, 107133 https://doi.org/10.1016/j.quascirev.2021.107133.
Wang, S., McNamara, S.M., Moore, C.W., Obrist, D., Steffen, A., Shepson, P.B., Staebler, R.M., Raso, A.R.W., Pratt, K.A., 2019. Direct detection of atmospheric atomic bromine leading to mercury and ozone depletion. Proc. Natl. Acad. Sci. USA 116, 14479–14484. https://doi.org/10.1073/pnas.1900613116.
Williamson, C.E., Zepp, R.G., Lucas, R.M., Madronich, S., Austin, A.T., Ballaré, C.L., Norval, M., Sulzberger, B., Bais, A.F., McKenzie, R.L., Robinson, S.A., Häder, D.-P., Paul, N.D., Bornman, J.F., 2014. Solar ultraviolet radiation in a changing climate. Nat. Clim. Change 4, 434–441. https://doi.org/10.1038/nclimate2225.